THE JOURNAL OF BIOLOGICAL CHEMISTRY VOL. 289, NO. 15, pp. 10853–10864, April 11, 2014

Regulation of Large Conductance Ca^{2+}-activated K^+ (BK) Channel β1 Subunit Expression by Muscle RING Finger Protein 1 in Diabetic Vessels*

Received for publication, September 24, 2013, and in revised form, February 23, 2014 Published, JBC Papers in Press, February 25, 2014, DOI 10.1074/jbc.M113.520940

Fu Yi[‡§1], **Huan Wang**[‡], **Qiang Chai**[‡], **Xiaoli Wang**[‡], **Win-Kuang Shen**[¶], **Monte S. Willis**[‖], **Hon-Chi Lee**[‡], **and Tong Lu**[‡2]

From the [‡]*Department of Internal Medicine, Mayo Clinic, Rochester, Minnesota 55905, the* [§]*Department of Cardiology, Xijing Hospital, Fourth Military Medical University, Xian 710032, China, the* [¶]*Department of Internal Medicine, Mayo Clinic, Scottsdale, Arizona 85259, and the* [‖]*Department of Pathology and Laboratory Medicine, University of North Carolina, Chapel Hill, North Carolina 27599*

Background: Impaired BK channel function in diabetic vessels is associated with decreased BK channel β1 subunit (BK-β1) expression.
Results: Muscle RING finger protein 1 (MuRF1) physically interacts with BK-β1 and accelerates BK-β1 proteolysis.
Conclusion: Increased MuRF1 expression is a novel mechanism underlying diabetic BK channelopathy and vasculopathy.
Significance: MuRF1 is a potential therapeutic target of BK channel dysfunction and vascular complications in diabetes.

The large conductance Ca^{2+}-activated K^+ (BK) channel, expressed abundantly in vascular smooth muscle cells (SMCs), is a key determinant of vascular tone. BK channel activity is tightly regulated by its accessory β1 subunit (BK-β1). However, BK channel function is impaired in diabetic vessels by increased ubiquitin/proteasome-dependent BK-β1 protein degradation. Muscle RING finger protein 1 (MuRF1), a muscle-specific ubiquitin ligase, is implicated in many cardiac and skeletal muscle diseases. However, the role of MuRF1 in the regulation of vascular BK channel and coronary function has not been examined. In this study, we hypothesized that MuRF1 participated in BK-β1 proteolysis, leading to the down-regulation of BK channel activation and impaired coronary function in diabetes. Combining patch clamp and molecular biological approaches, we found that MuRF1 expression was enhanced, accompanied by reduced BK-β1 expression, in high glucose-cultured human coronary SMCs and in diabetic vessels. Knockdown of MuRF1 by siRNA in cultured human SMCs attenuated BK-β1 ubiquitination and increased BK-β1 expression, whereas adenoviral expression of MuRF1 in mouse coronary arteries reduced BK-β1 expression and diminished BK channel-mediated vasodilation. Physical interaction between the N terminus of BK-β1 and the coiled-coil domain of MuRF1 was demonstrated by pull-down assay. Moreover, MuRF1 expression was regulated by NF-κB. Most importantly, pharmacological inhibition of proteasome and NF-κB activities preserved BK-β1 expression and BK-channel-mediated coronary vasodilation in diabetic mice. Hence, our results provide the first evidence that the up-regulation of NF-κB-dependent MuRF1 expression is a novel mechanism that leads to BK channelopathy and vasculopathy in diabetes.

Diabetes mellitus has become a global epidemic. In the United States, 25.8 million people have diabetes, and another 79 million Americans are prediabetic. These figures will more than double by 2030. Diabetes is an independent risk factor of vascular pathology and a leading cause of cardiovascular morbidity and mortality (1, 2). Major causes of vascular dysfunction in diabetes involve both endothelium-dependent and endothelium-independent mechanisms. There is a large body of evidence showing the abnormality of vascular smooth muscle function in diabetes. However, the underlying molecular mechanisms remain unclear (3–9).

The large conductance Ca^{2+}-activated K^+ (BK)[3] channels, densely populated in vascular smooth muscle cells (SMCs), play a negative feedback role in the regulation of vascular tone. BK channels are activated by the increase of intracellular free Ca^{2+} concentrations ($[Ca^{2+}]_i$) to generate spontaneous transient outward currents, which hyperpolarizes the membrane potential of vascular SMCs, inactivates voltage-dependent Ca^{2+} channels, and leads to vascular relaxation (8, 10–14). Functional vascular BK channels are octameric complexes with four BK-α and four BK-β1 subunits. BK-β1, encoded by the KCNMB1 gene, is a key determinant of BK channel electrophysiology, enhancing the BK-α sensitivity to Ca^{2+} and voltage and allowing channel activation in the physiological ranges of $[Ca^{2+}]_i$ and membrane potentials (15–18). Regulation of BK channel activity by many biological mediators, such as polyunsaturated fatty acids, thromboxane A2, and steroid hormones, are mediated through BK-β1 stimulation, demonstrating the

* This work was supported, in whole or in part, by National Institutes of Health Grants HL-74180 and HL-080118. This work was also supported by American Diabetes Association Grants ADA-JFA-07-39 and 1-12-BS-119).

[1] Supported by National Natural Science Foundation of the People's Republic of China Grant 81000686.

[2] To whom correspondence should be addressed: Div. of Cardiovascular Diseases, Dept. of Internal Medicine, Mayo Clinic, 200 First St. S.W., Rochester, MN 55905. Tel.: 507-255-9653; Fax: 507-538-6418; E-mail: lu.tong@mayo.edu.

[3] The abbreviations used are: BK, large conductance Ca^{2+}-activated K^+ channel; SMC, smooth muscle cell; UPS, ubiquitin proteasome system; MuRF1, muscle RING finger; IKK, IκB kinase; STZ, streptozotocin; DHS-1, dehydrosoyasaponin-1; NG, normal glucose; HG, high glucose; co-IP, co-immunoprecipitation; TPCA-1, 2-[(Aminocarbonyl)amino]-5-(4-fluorophenyl)-3-thiophenecarboxamide; Ad, adenovirus.

physiological importance of BK-β1 (19–22). The clinical relevance of BK-β1 is underscored by the findings that down-regulation of BK-β1 function contributes to hypertension and renal disease but that a gain-of-function mutation of BK-β1 is associated with a low prevalence of diastolic hypertension in humans (23–25). However, vascular BK channel function is impaired in both type 1 and type 2 diabetes mellitus and is an important ionic mechanism leading to diabetic vascular dysfunction. Current experimental evidence indicates that BK channel malfunction in diabetic vessels is associated with a significant down-regulation of BK-β1 protein expression, resulting in Ca^{2+} sparks/spontaneous transient outward current uncoupling and loss of Ca^{2+}-mediated channel activation even though the Ca^{2+} spark amplitude and $[Ca^{2+}]_i$ were increased in vascular SMCs of diabetes (8, 26–30). We have reported previously that *ex vivo* expression of the KCNMB1 gene in diabetic mouse coronary arteries rescued BK channel function and preserved normal coronary reactivity, suggesting that BK-β1 is an important molecular target for the treatment of diabetic vascular diseases (31). However, the molecular mechanisms that produce BK-β1 down-regulation have not been thoroughly delineated.

Protein homeostasis with a balanced regulation between syntheses and degradation is essential for normal cellular function. The ubiquitin proteasome system (UPS) is a major pathway of proteolysis, accounting for 80–90% of intracellular protein degradation in mammalian cells (32). This process is facilitated by three distinct enzymatic steps that involve an ubiquitin-activating enzyme (E1), an ubiquitin-conjugating enzyme (E2), and an ubiquitin ligase (E3). E1 activates ubiquitin, E2 accepts the transfer of activated ubiquitin, and E3 selects proteins for ubiquitination. Finally, the polyubiquitinated target proteins are degraded to short peptides in the 26 S proteasome (32). Of these, the E3 reaction is critical for the system because it recognizes the targeted substrates for ubiquitination and confers specificity of protein turnover. There are 617 E3 ligases functionally annotated in the human genome (33). The muscle RING finger (MuRF) protein family, comprised of three members (MuRF1, MuRF2, and MuRF3), is a group of muscle-specific E3s. All three isoforms are specifically expressed in cardiac and skeletal muscles and contain four important structures: a RING finger domain, a MuRF family conserved region, a "B-box" domain, and multiple coiled-coil domains (34). MuRF1, in particular, has been implicated in many heart diseases, including myocardial hypertrophy, myocardial atrophy, ischemia, heart failure, myocarditis, and familial cardiomyopathy (35, 36). Human genetic and functional studies have revealed the clinical significance of MuRF1, which confirmed that MuRF1 mutations cause hypertrophic cardiomyopathy in patients (37). However, the role of MuRF1 in vascular diseases is unclear.

The NF-κB complex is composed of the p65 (RelA), RelB, c-Rel, and p105/p50 (NF-κB1) or p100/p52 (NF-κB2) subunits. In unstimulated cells, p65 is bound to an inhibitory subunit (IκB) that keeps it sequestered in an inactive state in the cytoplasm. Phosphorylation of IκB by IκB kinase (IKK) leads to its dissociation from p65, which facilitates p65/p50 or p65/p52 dimeric complex nuclear translocation and promotes its transcriptional activity (38). In addition, the unbound phospho-IκB is degraded through the UPS. MuRF1 is one of the target genes regulated by NF-κB (39). In this study, we report that the MuRF1 physically interacted with BK-β1 and down-regulated BK-β1 expression through MuRF1-facilitated, UPS-dependent BK-β1 proteolysis. MuRF1 expression was controlled by NF-κB, which is up-regulated in diabetic vessels, leading to acceleration of BK-β1 proteolysis. Most importantly, knockdown of MuRF1 or inhibition of proteasome and NF-κB activities significantly enhanced BK-β1 expression, restored vascular BK channel activity, and preserved coronary function in diabetes. Our results identified a fundamental mechanism that underlies diabetic BK channelopathy and vasculopathy. Therefore, MuRF1 is a potential novel target for the treatment of vascular complications in diabetes.

EXPERIMENTAL PROCEDURES

STZ-induced Diabetic Mice—Male mice (strain C57BL/CJ) 4 weeks of age were purchased from The Jackson Laboratory (Bar Harbor, ME). Animals were made diabetic by an injection of STZ (100 mg/kg body weight, intraperitoneally). Animals with blood glucose >300 mg/dl were considered diabetic and were used for experiments 8 weeks after developing hyperglycemia. All protocols were approved by the Institutional Animal Care and Use Committee of the Mayo Clinic, Rochester, MN.

Coronary Artery SMC Isolation—Mouse coronary SMCs were isolated enzymatically as described previously (40). In brief, the coronary arteries were carefully dissected in ice-cold dissociation buffer (145 mM NaCl, 4.0 mM KCl, 0.05 mM $CaCl_2$, 1.0 mM $MgCl_2$, 10 mM HEPES, and 10 mM glucose (pH 7.2)). The vessels were placed in dissociation buffer containing 0.1% w/v BSA and incubated in a shaking water bath at 37 °C for 3 min. The vessels were incubated with fresh 0.1% w/v BSA dissociation buffer containing 1.5 mg/ml papain and 1.0 mg/ml dithiothreitol in a shaking water bath at 37 °C for another 3 min. This was followed by digestion in fresh 0.1% w/v BSA dissociation buffer containing 1.0 mg/ml collagenase and 1.0 mg/ml of trypsin inhibitor at 37 °C for 3 min. The vessels were stored in 2 ml of dissociation buffer triturated gently with a fire-polished glass pipette until the cells were completely dissociated.

BK Channel Current Recordings—Single channel currents were elicited at +60 mV from inside-out excised membrane patches using an Axopatch 200B (Axon Instruments, Inc.) (27, 31, 41). The output signals were filtered with an 8-pole Bessel filter (902 LPF, Frequency Devices, Inc.) at 5 kHz and digitized at 50 kHz. Patch pipettes had a typical tip resistance of 5–10 MΩ when filled with the pipette solution, which contained 140 mM KCl, 1 mM $CaCl_2$, 1 mM $MgCl_2$, 1 mM EGTA, and 10 mM HEPES (pH 7.4) with KOH. The bath solution contained 140 mM KCl, 1 mM $MgCl_2$, 1 mM EGTA, 0.465 mM $CaCl_2$ (0.2 μM free Ca^{2+}, calculated using Chelator software), and 10 mM HEPES (pH 7.35) with KOH. The inside-out single BK currents were determined by its unitary current amplitude (*i*) and sensitivity to free Ca^{2+} concentrations, as described previously (41). Normalized channel open probability (NP_o) was determined by the following equation (42):

$$NP_o = \sum(t_n n)/T \quad \text{(Eq. 1)}$$

where t represents the open time of a channel obtained at a distinct level (n), and T is the total recording time.

The effects of dehydrosoyasaponin-1 (DHS-1, a BK-β1-specific activator) on BK channel open probability (P_o) were measured in the same membrane patch before and after drug application to the cytoplasmic surface. After the DHS-1 experiments were completed, the total number of channels in each membrane preparation was determined by exposure to 10 μM Ca^{2+} that activates all channels in the patch and produces the maximal BK channel P_o in coronary SMCs (41). All patch clamp experiments were performed at room temperature (22–24 °C). Data analysis was performed using Clampfit 10.2 software (Axon Instruments, Inc.).

Cell Culture, Subcloning, Site-directed Mutagenesis, cDNA Transfection, Adenoviral Gene Transduction, and mRNA Knockdown—Mouse MuRF1 WT with a Myc tag in the N terminus (Myc-MuRF1 WT, amino acids 1∼351) (accession no. DQ229108), the RING finger deletion mutant (Myc-MuRF1ΔR, amino acids 79∼351), the family conserved region deletion mutant (Myc-MuRF1ΔFMC, amino acids 100∼351), and the B-box deletion mutant (Myc-MuRF1ΔB, amino acids 160∼351) cDNAs in pCMV Tag3B as well as an adenovirus carrying MuRF1 (Ad-MuRF1) and the GFP gene (Ad-GFP) were prepared by Dr. Monte S. Willis (University of North Carolina at Chapel Hill). Myc-MuRF1ΔB with deletion of the last 10 C-terminal amino acid residues (Myc-MuRF1ΔBΔC, amino acids 160∼340) was created by introducing a stop codon using the QuikChange site-directed mutagenesis kit (Stratagene, Inc.) (43).

Human BK-β1 WT cDNA (amino acids 1∼191) (accession no. MN_004137.3) was subcloned into pIRES2-EGFP with two FLAG tags in the N-terminal of BK-β1 (28). Three FLAG-BK-β1 truncation mutants, the N-terminal mutant (amino acids 1∼39), the transmembrane domain mutant (amino acids 15∼179), and the C-terminal mutant (amino acids 155∼191) were also constructed. The orientations of the constructs and the correctness of the mutation were verified by DNA sequencing (DNA Facility Core of the Mayo Clinic, Rochester, MN). MuRF1 siRNA and control siRNA were obtained from Santa Cruz Biotechnology, Inc. HA-tagged human ubiquitin (HA-ubiquitin) in pcDNA3 was obtained from Addgene, Inc. cDNAs and siRNA transfection were conducted using a Lipofectamine 2000 transfection kit (Invitrogen). The aortas and coronary arteries of mice were transduced with Ad-MuRF1 and Ad-GFP at 1×10^{11} particles/ml for 12 h (28, 31).

HEK293 cells were cultured in DMEM. Primary human coronary SMCs were purchased from Lonza Walkersville, Inc. and were cultured with Clonetics SmBM (Lonza Walkersville, Inc.) containing 5 mM glucose (normal glucose, NG) or 22 mM glucose (high glucose, HG). All experiments were performed using cells between passages 4 and 5.

Videomicroscopy—Vasoreactivity was measured as described previously (31, 44). Isolated mouse coronary arteries (1–2 mm in length and 80–130 μm in diameter) were mounted in a vessel chamber filled with Krebs solution containing 118.3 mM NaCl, 4.7 mM KCl, 2.5 mM $CaCl_2$, 1.2 mM $MgSO_4$, 1.2 mM KH_2PO_4, 25 mM $NaHCO_3$, and 11.1 mM glucose (pH 7.4) and were secured between two borosilicate glass micropipettes with a 10-O ophthalmic suture. The lumen of each vessel was filled with Krebs solution through the micropipettes and maintained at a constant pressure (no flow) of 60 mm Hg, followed by equilibration for 60 min in oxygenated (20% O_2 + 5% CO_2 balanced with N_2, 37 °C) Krebs solution. The vessels were deemed unacceptable for experiments if they demonstrated leaks or failed to produce more than a 50% constriction to graded doses of endothelin-1. The endothelium was denuded by slowly perfusing 3–5 ml of air through the lumen of unpressurized vessels. The effectiveness of endothelium denudation was verified by demonstrating that the vessel failed to dilate to 1 μM acetylcholine, constricted normally to ET-1, and dilated normally to 100 μM sodium nitroprusside. Concentration-response relationships of NS-1619 (10^{-9}-10^{-5} M) on vasodilatation were measured, and comparisons were made in mouse coronary arteries 12 h after transduction with Ad-GFP, Ad-MuRF1, or Ad-MuRF1 in the presence of 10 μM MG132. At the end of each experiment, vessels were maximally dilated with a Ca^{2+}-free solution, and the percentage of dilatation in response to NS-1619 was normalized to the maximal diameter.

Coimmunoprecipitation (Co-IP) and Western Blot Analysis—Co-IP was performed as described previously (40). Transfected HEK293 cells were washed with PBS three times. The aortas or collected cells were incubated with 200 μl of radioimmune precipitation assay buffer (50 mM Tris, 150 mM NaCl, 1 mM NaF_2, 1 mM EDTA, 1 mM EGTA, 1 mM $NaVO_4$, and 1% Triton X-100 (pH 7.5)) and 1 μl of protease inhibitor on ice for 30 min, homogenized, and then centrifuged at 8000 rpm at 4 °C for 10 min. The supernatant (about 200 μg in 200 μl) was incubated with anti-HA (Sigma-Aldrich) or anti-FLAG (Cell Signaling Technology, Inc.) antibodies at a final concentration of 4 μg/ml for each at 4 °C overnight. The samples were then incubated with 20 μl protein G Plus-agarose (Santa Cruz Biotechnology, Inc.) at 4 °C for 2 h with rotation. After centrifugation at 1000 rpm for 7 min and washing twice with radioimmune precipitation assay/protease inhibitor buffer, the immunoprecipitates were collected and eluted from agarose with 30 μl of SDS-PAGE loading buffer/tube.

Blots were probed against anti-BK-α (1:50, University of California at Davis), anti-BK-β1 (1:200, customer-made) (28, 31), anti-MuRF1 (1:200, ECM Biosciences, LLC), anti-NF-κB/p105 (Cell Signaling Technology Inc.), anti-p65 (Cell Signaling Technology Inc.), anti-IκB (1:200, Abcam), anti-FLAG (1:2000, Sigma-Aldrich), anti-HA (1:2000, Sigma-Aldrich), anti-Myc (1:2000, Sigma-Aldrich), and anti-ubiquitin (1:100, Santa Cruz Biotechnology, Inc.) antibodies. Protein expression was expressed as relative abundance normalized to β-actin or GAPDH (1:2000, Sigma-Aldrich). Optical density of the bands was analyzed using Scion Image software (Scion).

Size Exclusion Chromatography—Chromatographic separation of FLAG-BK-β1(1–39) and Myc-MuRF1 mutant proteins was performed by the Mayo Clinic Proteomics Center (Rochester, MN) using a Superdex 75 10/300 column (GE Healthcare). Samples (350 μl) were equilibrated in radioimmune precipitation assay buffer and run through the size exclusion column with a flow rate of 0.4 ml/min. 48 fractions (0.4 ml each) were collected. Standard proteins with known molecular weights (Gel Filtration Standards, Bio-Rad Laboratories) in

phosphate-buffered saline were run under the same conditions. The presence of FLAG-BK-β1 and Myc-MuRF1 proteins in each fraction (30 μl) were measured using Western blot analyses, and the band intensities were plotted against standard protein peaks (bovine thyroglobulin, 670 kDa; bovine IgG, 158 kDa; chicken ovalbumin, 44 kDa; horse myoglobin, 17 kDa, and Vitamin B_{12}, 1350 Da) to estimate the size of proteins.

Chemicals—2-[(Aminocarbonyl)amino]-5-(4-fluorophenyl)-3-thiophenecarboxamide (TPCA-1) was purchased from Tocris Bioscience Co. Unless mentioned otherwise, all other chemicals were obtained from Sigma-Aldrich.

Statistical Analysis—All data are expressed as mean ± S.E. Student's *t* test was employed to compare data between two groups, and a paired *t* test was used to compare data before and after treatment. One-way analysis of variance followed by the Tukey test analysis was used to compare multiple groups using SigmaStat software (Jandel Scientific Software, Inc.). A statistically significant difference was defined as $p < 0.05$.

RESULTS

Type 1 Diabetic Mice—Male mice at 4 weeks of age received a single dose of STZ (100 mg/kg body weight, intraperitoneally), whereas controls received saline injections. Eight weeks after injection, the average body weights and blood glucose levels were 28.05 ± 0.82 g ($n = 30$) and 181.43 ± 5.32 mg/dl ($n = 30$) in control mice and 23.61 ± 0.88 g ($n = 30$, $p < 0.05$ *versus* control) and 466.22 ± 18.05 mg/dl ($n = 30$, $p < 0.05$ *versus* control) in diabetic mice, respectively. Hence, STZ-induced diabetic mice had a 15.8% decrease in body weight and a 157.0% increase in blood glucose level.

Diminished BK-β1-mediated BK Channel Activation and Reduced BK-β1 Protein Expression in Vascular SMCs from Diabetic Mice and in Human Coronary SMCs Cultured with HG—Inside-out single BK channel currents were recorded from the freshly isolated coronary SMCs of control and diabetic mice. BK channel NP_o at baseline was 0.19 ± 0.07 ($n = 11$) in control SMCs and was reduced significantly in diabetic SMCs (0.01 ± 0.004, $n = 11$, $p < 0.05$ *versus* control). The BK-β1-mediated channel activation was determined by cytoplasmic exposure to 0.1 μM DHS-1 (a BK-β1-specific activator), which resulted in a 5.5-fold increase in NP_o (1.10 ± 0.30, $n = 11$, $p < 0.05$ *versus* baseline) in control mice. In diabetic coronary SMCs, there was a small but significant increase in response to DHS-1 stimulation (0.05 ± 0.01, $n = 11$, $p < 0.05$ *versus* diabetic baseline) (Fig. 1*A*). Fig. 1*B* (*left panel*) represents a full-lane Western blot analysis of anti-ubiquitin antibody against the lysates of control and diabetic mouse aortas and shows an increase of total ubiquitinated proteins in diabetic aortas. To determine and compare the level of ubiquitinated BK-β1 protein in control and diabetic vessels, we performed a pulldown assay of control and diabetic mouse aortas with anti-BK-β1 antibodies, followed by Western blotting against anti-ubiquitin antibody. There was a 1.56 ± 0.28-fold increase in BK-β1 ubiquitination in diabetic aortas ($n = 4$, $p < 0.05$ *versus* control) (Fig. 1*B*, *right panel*). Importantly, BK-β1 expression was down-regulated by 0.51 ± 0.13-fold ($n = 3$, $p < 0.05$, *versus* control) in diabetic mouse aortas, accompanied by a 2.83 ± 0.16-fold increase in MuRF1 expression ($n = 3$, $p < 0.05$, *versus* control) (Fig. 1*C*). Similar results were observed in human coronary SMCs after a 2-week culture with HG, where BK-β1 expression was 0.60 ± 0.05-fold lower and MuRF1 expression was 1.84 ± 0.21-fold higher than cells cultured with NG ($n = 3$, $p < 0.05$ in both) (Fig. 1*D*). Note that the changes in protein expression profiles in HG culture conditions were not due to osmolality of culture mediums under our experimental conditions because human coronary SMCs cultured with 5 mM glucose plus 17 mM mannitol did not alter the protein levels of BK-β1 and MuRF1 compared with those cultured with NG alone (data not shown). In addition, we have shown that the BK-β1 mRNA level was not reduced in STZ-induced diabetic vessels or in HG-cultured human coronary SMCs (28). Hence, the impaired BK channel function in diabetes is most likely due to accelerated BK-β1 degradation from increased MuRF1 expression.

Regulation of BK-β1 Expression and Vascular BK Channel Function by MuRF1—To confirm the role of MuRF1 in the regulation of BK-β1 expression, we examined the level of BK-β1 protein expression in HG-cultured human coronary SMCs transfected with MuRF1 siRNA or with control siRNA. 48 h after transfection with 0.1 μM MuRF1 siRNA, MuRF1 expression was down-regulated by 76.1 ± 5.9% ($n = 3$, $p < 0.05$ *versus* control siRNA), whereas that of BK-β1 was augmented by 86.1 ± 14.7% ($n = 3$, $p < 0.05$ *versus* control siRNA) (Fig. 2*A*). Knockdown of MuRF1 preserved BK-β1 protein expression to a level similar as that in NG-cultured cells.

Fig. 2*B* shows HEK293 cells stably expressing FLAG-BK-β1 WT 48 h after transient expression with Myc-MuRF1 WT or Myc-MuRF1ΔR (an inactive mutant with the RING structure deletion). There was a 2.58 ± 0.14-fold increase in BK-β1 expression ($n = 3$, $p < 0.05$) in the cells expressing Myc-MuRF1ΔR compared with the cells expressing Myc-MuRF1 WT. However, coexpression of Myc-MuRF1 WT did not change the protein level of BK-α stably expressed in HEK293 cells. Moreover, cotransfection of HA-ubiquitin with Myc-MuRF1 WT produced a 5-fold increase in ubiquitinated BK-β1 protein in the immunoprecipitates against anti-HA antibody or anti-FLAG antibody compared with those in the cells with HA-ubiquitin and Myc-MuRF1ΔR cotransfection (Fig. 2*C*).

The role of MuRF1 on the regulation of vascular BK channel activity and coronary vasoreactivity was further demonstrated by adenoviral-mediated overexpression of MuRF1 (Ad-MuRF1) in control mouse arteries. As shown in Fig. 3*A*, there was a 177.2 ± 11.5% ($n = 3$) increase of MuRF1 expression and a 66.8 ± 15.6% decrease of BK-β1 expression in mouse aortas 12 h after transduction with Ad-MuRF1 compared with control transduction with adenovirus carrying the GFP gene (*Ad-GFP*) (Fig. 3*A*). Patch clamp studies confirmed that BK channel activation by 0.1 μM DHS-1 was diminished in mouse coronary SMCs 12 h after transduction with Ad-MuRF1, which was accompanied by impaired coronary vasodilation in response to NS1619 (a BK channel activator). The DHS-1-mediated BK channel activation and the NS1619-induced (10^{-9}-10^{-5} M) vasodilation were intact in coronary arteries with Ad-GFP transduction (Fig. 3, *B* and *C*). Moreover, the inhibitory effect of Ad-MuRF1 on coronary vasoreactivity was abrogated by a 12-h

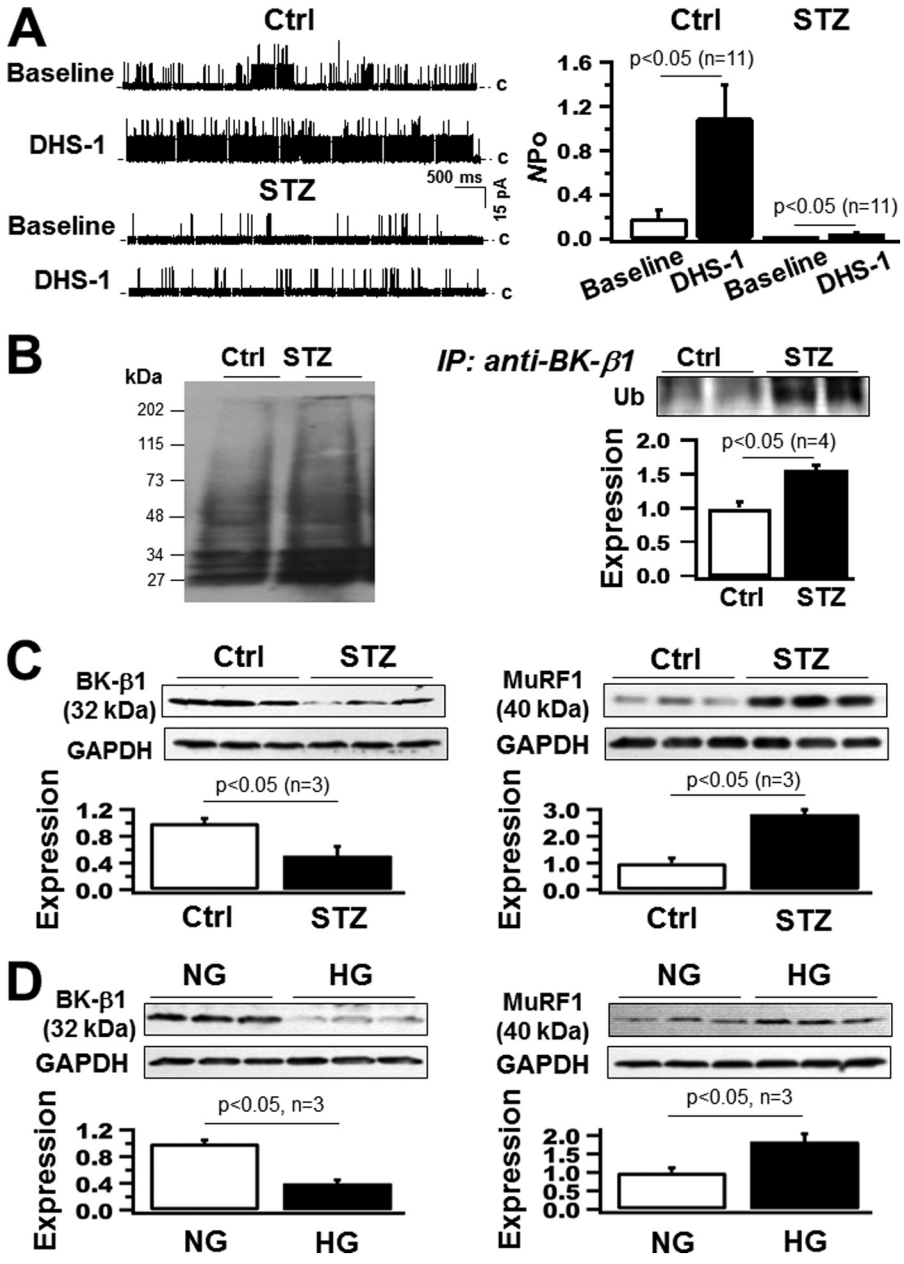

FIGURE 1. **Impaired BK-β1-mediated channel activation, reduced BK-β1 expression, and increased MuRF1 expression in diabetic vessels and in HG-cultured human coronary SMCs.** *A*, inside-out single-channel BK currents were elicited at +60 mV in freshly isolated coronary SMCs from control and diabetic mice before and after exposure to DHS-1 (0.1 μM). DHS-1 robustly increased BK channel NP_o in control SMCs, but its effects were diminished in diabetic SMCs. *Dashed lines* represent the channel closed state (*c*). *B*, *left panel*, the cell lysates of control and diabetic mouse aortas were blotted against anti-ubiquitin antibody. *Right panel*, the immunoprecipitates (*IPs*) of anti-BK-β1 antibodies were blotted against anti-ubiquitin (*Ub*) antibody, showing a significant increase of ubiquitinated BK-β1 protein in diabetic mice. *Ctrl*, control. *C* and *D*, a marked reduction of BK-β1 expression in the aortas of diabetic mice compared with those of control mice and in human coronary SMCs after a 2-week culture with 22 mM glucose (*HG*) compared with that with 5 mM glucose (*NG*) culture. Group data with statistical analysis are shown in the *bar graphs*.

treatment with 10 μM MG132 (a proteasomal inhibitor) (Fig. 3*C*). Our results confirmed that MuRF1 reduced BK-β1-mediated channel activation and impaired coronary vasodilation through MuRF1-dependent BK-β1 protein ubiquitination and protein turnover.

Functional Regions of BK-β1 and MuRF1 Protein Complex Formation—To gain further understanding on interaction between BK-β1 and MuRF1, we constructed a series of FLAG-BK-β1 truncation mutants, as shown in Fig. 4*A*. We coexpressed Myc-MuRF1 WT with individual FLAG-BK-β1 truncation mutants in HEK293 cells. The immunoprecipitates pulled down by anti-Myc antibody from the cell lysates were blotted against anti-FLAG antibody. As shown in Fig. 4*A*, the co-IP with MuRF1 was detected only when the N-terminal segment of BK-β1(1–39) was present. Similarly, the domains in MuRF1 for BK-β1 interaction were determined by coexpression of FLAG-BK-β1 WT with individual Myc-MuRF1 mutants: Myc-MuRF1ΔR, Myc-MuRF1ΔMFC, Myc-MuRF1ΔB, and Myc-MuRF1ΔBΔC (Fig. 4*B*). When the immunoprecipitates of anti-FLAG antibody were blotted against anti-Myc antibody, the co-IP with BK-β1 was found in MuRF1 WT, MuRF1ΔB, and MuRF1ΔBΔC mutants, indicating that the

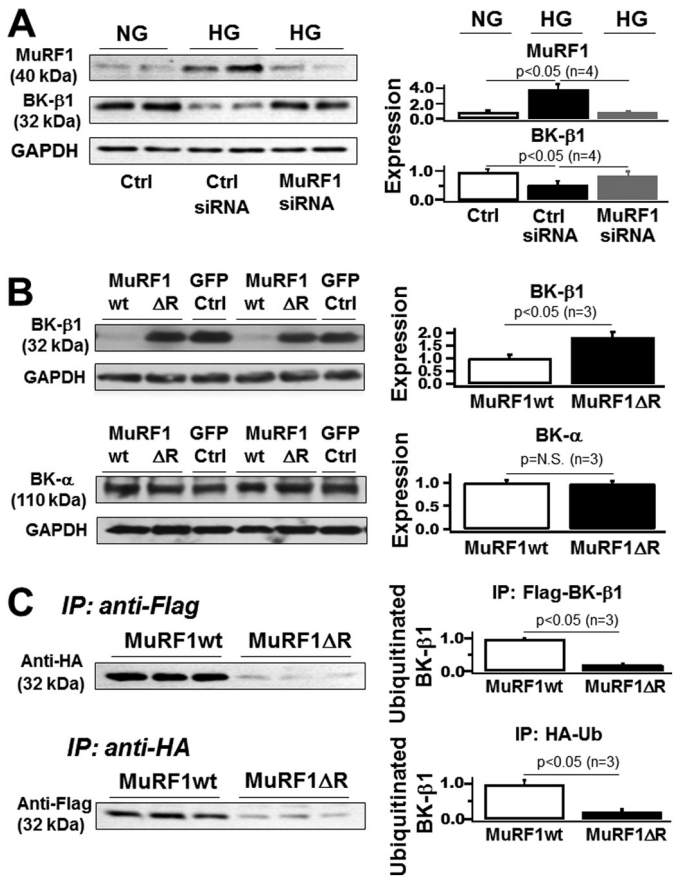

FIGURE 2. **Regulation of BK-β1 expression by MuRF1.** *A*, after a 2-week culture in NG or HG, BK-β1 protein expression in human coronary SMCs was determined under the following conditions: NG culture alone, HG culture after a 48-h transfection with control siRNA (0.1 μM), and HG culture after a 48-h transfection with MuRF1 siRNA (0.1 μM). MuRF1 siRNA suppressed MuRF1 expression under HG culture conditions to that of NG culture conditions. *Ctrl*, control. *B*, FLAG-BK-β1 or FLAG-BK-α stably expressed in HEK293 cells 48 h after cotransfection with Myc-MuRF1 WT cDNA or Myc-MuRF1ΔR mutant cDNA. The BK-β1 protein level was halved in cells with MuRF1 WT transfection, but BK-α expression remained unchanged. *N.S.*, not significant. *C* and *D*, coimmunoprecipitation experiment shows attenuated BK-β1 protein ubiquitination in the pulldown complexes with anti-HA-ubiquitin (*anti-HA-Ub*) antibodies or with anti-FLAG antibodies in HEK293 cells after a 24-h transfection with MuRF1ΔR compared with those with MuRF1 WT. Group data with statistical analysis are shown in the *bar graphs*.

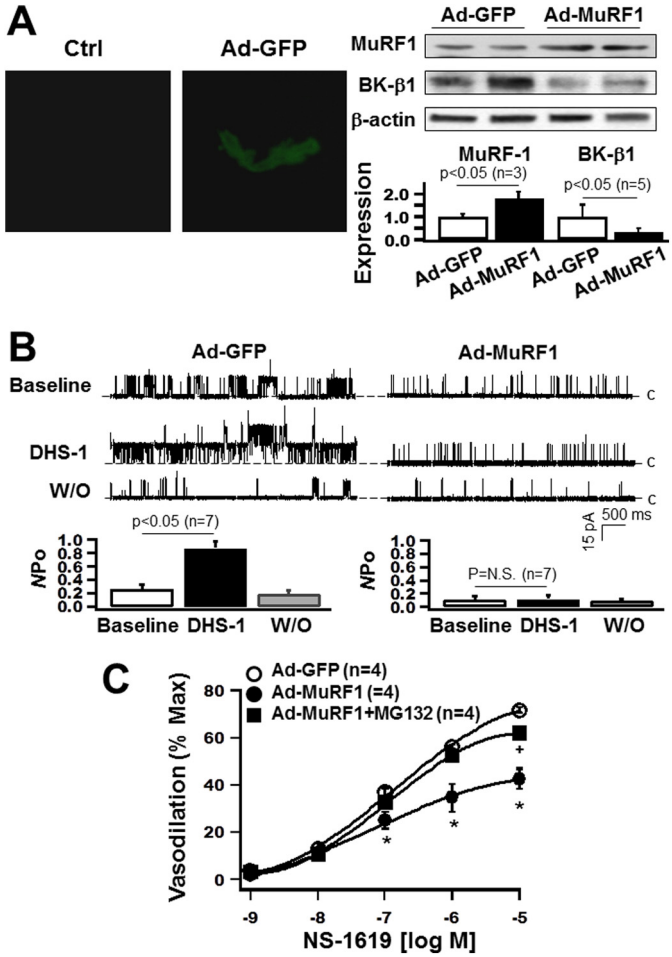

FIGURE 3. **Reduced BK-β1 expression and BK-β1-mediated channel activation in vascular SMCs by MuRF1 expression.** *A*, fluorescence microscopy images illustrate GPF expression in endothelially denudated mouse coronary artery 12 h after transduction with Ad-GFP but not in a negative control artery. Immunoblot analyses show increased MuRF1 and decreased BK-β1 expression in the aortas of control (*Ctrl*) mice after a 12-h transduction with Ad-MuRF1 compared with controls with Ad-GFP transduction. *B*, inside-out single BK currents were elicited from +60 mV at baseline, after exposure to 0.1 μM DHS-1, and after washout (*W/O*). DHS-1 had no effect on mouse coronary SMCs 12 h after transduction with Ad-MuRF1. *Dashed lines* represent the channel closed state (*c*). Group data with statistical analysis are shown in the *bar graphs*. *N.S.*, not significant. *C*, effects of Ad-MuRF1 transduction on dose-dependent, NS1619-mediated (10^{-9}-10^{-5} M) dilation of endothelium-denuded coronary arteries from non-diabetic mice. Transduction with Ad-MuRF1 (12 h) attenuated the NS1619-induced vasodilation, but the NS1619 response was preserved in Ad-MuRF1-treated coronaries by incubation with MG132 (10 μM, 12 h). Control vessels received Ad-GFP transduction. *, $p < 0.05$, Ad-MuRF1 *versus* Ad-GFP; +, $p < 0.05$ Ad-MuRF1+MG132 *versus* Ad-GFP.

coiled-coil region of MuRF1 is essential for the interaction with BK-β1 (Fig. 4*B*). Interestingly, BK-β1 did not coimmunoprecipitate with MuRF1ΔR and MuRF1ΔMFC where the coiled-coil region is present, suggesting that the MuRF1-BK-β1 interaction is complex and may be influenced by additional factors.

To confirm that the protein-protein interaction was not due to nonspecific protein aggregation, we further performed size exclusion chromatography separations of FLAG-BK-β1(1–39) and Myc-MuRF1ΔBΔC mutants. A 48-h after transfection with a plasmid carrying FLAG-BK-β1(1–39) or Myc-MuRF1ΔBΔC (160–340) in HEK293 cells, respectively, the cell lysates were separated by a size exclusion column, and 48 fractions (0.4 ml each) were collected. Fig. 5*A* shows the protein expression of FLAG-BK-β1(1–39) and Myc-MuRF1ΔBΔC in the fractions of size exclusion chromatography. FLAG-BK-β1(1–39) was detected only in fractions 23∼26 with a molecular size about 17 kDa (Fig. 5*A*, *top panel*). The Myc-MuRF1ΔBΔC mutant was present in a fraction of 23∼25, with a molecular size about 27 kDa (Fig. 5*A*, *bottom panel*). The relative density of protein expression plotted against equivalent fractions is illustrated in Fig. 5*B*. Five protein standards with different molecular weights were separated under the same running conditions (*green line*). The distribution of FLAG-BK-β1(1–39) (*black line*) was coeluted with the molecular size standard of horse myoglobin of 17 kDa. There was a slight left shift in Myc-MuRF1ΔBΔC density distribution between the molecular size standard of horse myoglobin and chicken ovalbumin (44 kDa). An immunofluorescence experiment confirmed that FLAG-BK-β1(1–39) expressed on the membrane of HEK293 cells (data not shown). Taken together,

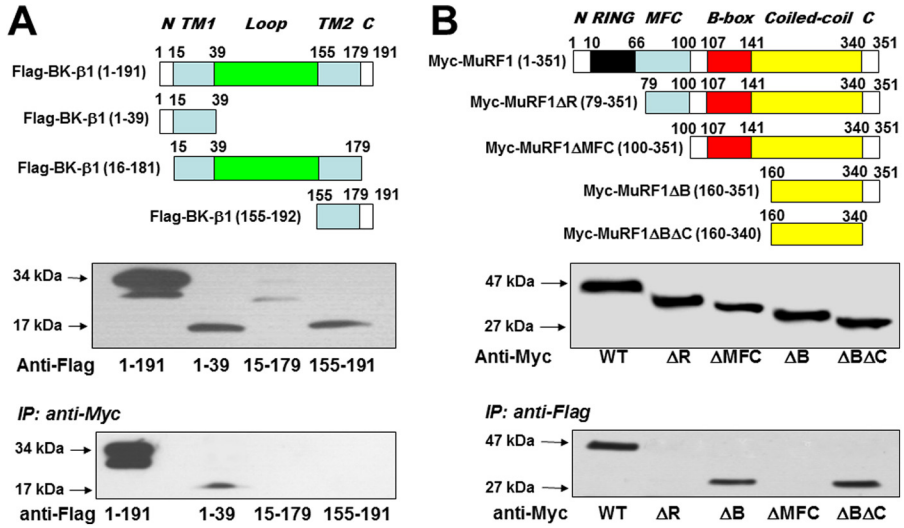

FIGURE 4. **The N terminus of BK-β1 physically interacts with the coiled-coil region of MuRF1.** *A*, schematic and protein expression of FLAG-tagged BK-β1 WT and its truncation mutants. The molecular sizes of BK-β1 WT and individual mutants are shown in immunoblot analyses. Immunoprecipitates pulled down by anti-Myc antibody were blotted against anti-FLAG antibody, showing that BK-β1 WT and BK-β1(1–39) proteins interacted with MuRF1 WT proteins. *B*, the constructs and protein expressions of Myc-MuRF1 WT and the truncation mutants. Immunoprecipitates from anti-FLAG antibodies were blotted against anti-Myc antibody. BK-β1 was only detected in Myc-MuRF1WT, Myc-MuRF1ΔB, and Myc-MuRF1ΔBΔC mutants but not in MuRF1ΔR and MuRF1ΔMFC mutants. These results suggest that the coiled-coil region of MuRF1 is necessary for the interaction with the N-terminal of BK-β1 but that the RING-finger domain and the family conserved region of MuRF1 may also affect the association between MuRF1 and BK-β1 proteins.

these results suggest that the proteins of FLAG-BK-β1(1–39) and MuRF1ΔBΔC were properly folded and that the pulldowns of BK-β1(1–39) and MuRF1ΔBΔC were not due to nonspecific protein aggregation.

We also performed size exclusion chromatography separation and immunoblot analysis in Myc-MuRF1ΔR and Myc-MuRF1ΔMFC mutants to determine whether the absence of FLAG-BK-β1 interaction was caused by protein misfolding because of the deletions. Myc-MuRF1ΔR and Myc-MuRF1ΔMFC proteins were present in fractions 20~22 (~40 kDa) and 21~23 (~34 kDa), respectively, similar to those we had predicted (data not shown). Hence, a lack of protein interaction between FLAG-BK-β1 and Myc-MuRF1ΔR or Myc-MuRF1ΔMFC is unlikely because of a nonspecific interaction with other proteins.

Inhibition of Proteasomal Activity Enhanced BK-β1 Expression and Restored the β1-mediated BK Channel Activation in Diabetic Vessels—To determine whether inhibition of proteasomal activity enhances BK channel function in diabetes, we measured vascular BK-β1 expression and BK channel activation by DHS-1 in diabetic mouse vessels. After a 24-h incubation with 10 μM MG132, BK-β1 expression in aortas was 2.46 ± 0.19-fold ($n = 3$, $p < 0.05$) higher than in untreated diabetic vessels (Fig. 6*A*). Patch clamp studies confirmed that BK channel openings at the baseline were significantly higher in freshly isolated coronary SMCs of diabetic mice after treatment with MG132 ($NP_o = 0.25 \pm 0.10$, $n = 11$) compared with diabetic cells without treatment ($NP_o = 0.018 \pm 0.004$, $n = 11$, $p < 0.05$ *versus* MG132 treatment). Importantly, activation of BK channel by 0.1 μM DHS-1 was robust in diabetic SMCs after a 12-h treatment with MG132 ($NP_o = 1.55 \pm 0.14$ of MG132 treatment, $n = 11$, $p < 0.05$ *versus* 0.048 ± 0.016 without MG132 treatment, $n = 11$, $p < 0.05$), whereas DHS-1 had no significant effects in diabetic cells without MG132 treatment (Fig. 6*B*). Hence, DHS-1 increased the NP_o 6.2-fold in MG132-treated cells compared with a 2.7-fold enhancement in the cells without MG132 treatment.

Regulation of MuRF1 Expression by NF-κB in Diabetic Vessels and in Human Coronary SMCs with HG Culture—Fig. 7*A* shows that the protein expression of the NF-κB1/p105, NF-κB1/p50 and p65 subunits from the aortas of diabetic mice was increased 1.36 ± 0.05-fold ($n = 3$), 2.53 ± 0.51-fold ($n = 3$), and 2.49 ± 0.25-fold ($n = 3$), respectively, compared with those from controls ($p < 0.05$ for all three). To further determine the role of NF-κB in MuRF1 and BK-β1 expression, we treated NG- and HG-cultured human coronary SMCs with 0.5 μM TPCA-1 (a selective IKK2 inhibitor) (Fig. 7*B*). In NG-cultured cells, 24-h TPCA-1 treatment significantly attenuated NF-κB1/p105 and NF-κB1/p50 expression 0.58 ± 0.06-fold and 0.81 ± 0.06-fold, respectively ($n = 4$, $p < 0.05$ *versus* controls for both), whereas IκB-β expression was increased 5.66 ± 0.78-fold ($n = 4$, $p < 0.05$ *versus* controls). Moreover, TPCA-1 treatment produced a 0.86 ± 0.01-fold reduction ($n = 4$, $p < 0.05$ *versus* controls) in MuRF1 expression without a significant change in BK-β1 protein level. In HG-cultured cells, IκB-β expression was 0.29 ± 0.27-fold lower than that in NG cells ($n = 4$, $p < 0.05$) and was associated with a 1.54 ± 0.19-fold increase in MuRF1 and a 0.61 ± 0.06-fold reduction in BK-β1 expression ($n = 4$, $p < 0.05$ *versus* NG in both). TPCA-1 treatment reduced NF-κB1/p105 and NF-κB1/p50 0.34 ± 0.11-fold and 0.59 ± 0.04-fold, respectively ($n = 4$, $p < 0.05$ *versus* HG in both) and enhanced IκB-β expression 24.8 ± 0.89-fold ($n = 4$, $p < 0.05$ *versus* HG), resulting in a 0.56 ± 0.09-fold decrease in MuRF1 expression and a 1.70 ± 0.13-fold increase in BK-β1 expression ($n = 4$, $p < 0.05$ *versus* HG in both). Hence, by reducing the active components of NF-κB1/50 and p65 and augmenting the expression of IκB-β expression, TPCA-1 abolished NF-κB/MuRF1-mediated BK-β1 degradation and protected BK-β1 protein level in HG-cultured cells.

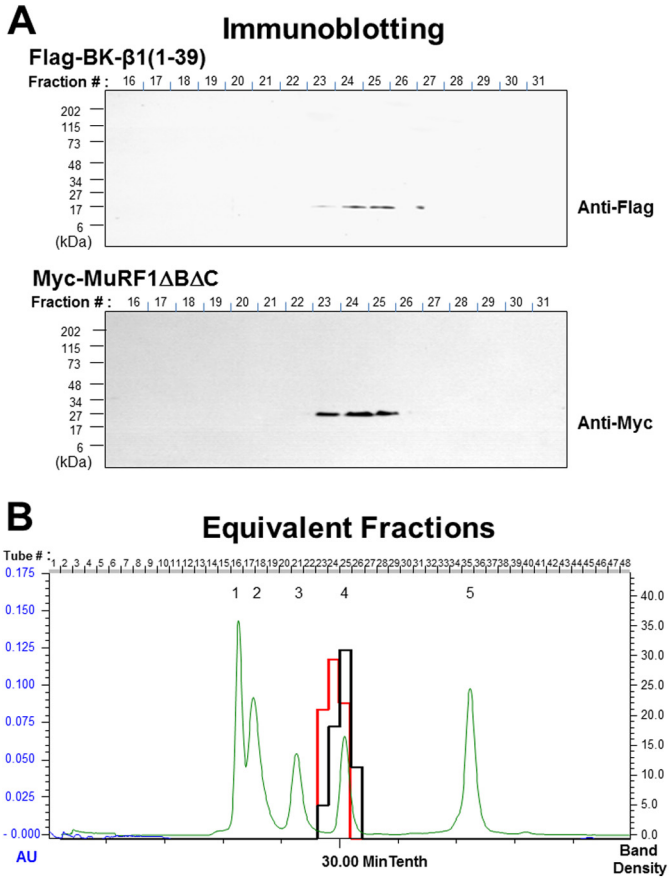

FIGURE 5. **Size exclusion chromatography separation of the FLAG-BK-β1(1–39) and Myc-MuRF1ΔBΔC mutations.** *A*, after 48 h of transfection of a vector containing FLAG-BK-β1(1–39) or Myc-MuRF1ΔBΔC mutants in HEK293 cells, cells were homogenized. 350 μl of cell lysates was loaded onto a size exclusion column (Sephadex 75 10/300 column, 10 × 30 cm, bed volume = 23.5 ml) at a flow rate of 0.4 ml/min. Forty-eight fractions of 0.4 ml each were collected. Immunoblot analyses show that FLAG-BK-β1(1–36) was detected in fractions 23∼26 with an estimated size of 17 kDa (*top panel*) and that Myc-MuRF1ΔBΔC was present in fractions 23∼25 with an estimated molecule weight about 27 kDa. *B*, the distributions of FLAG-BK-β1(1–39) (*black line*) and Myc-MuRF1ΔBΔC (*red line*) protein expression with protein markers (*green line*). Five protein standards with different molecular weights were separated under the same running conditions: *1*, bovine thyroglobulin, 670 kDa; *2*, bovine IgG, 158 kDa; *3*, chicken ovalbumin, 44 kDa; *4*, horse myoglobin, 17 kDa; and *5*, vitamin B_{12}, 1.35 kDa. *AU:* UV absorbance at 280 nm.

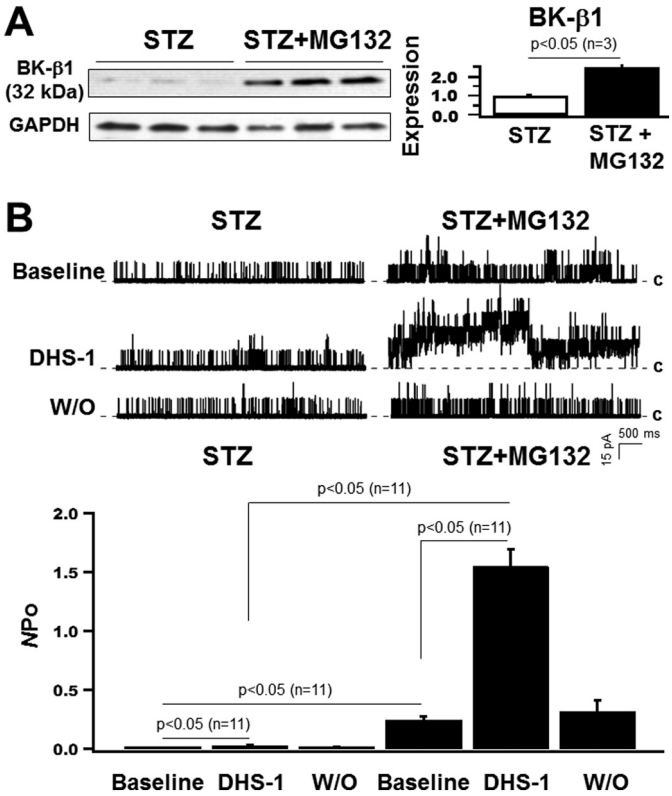

FIGURE 6. **Enhanced BK-β1 expression and BK-β1-mediated channel activation by MG132.** *A*, protein expression of BK-β1 in STZ-induced diabetic aortas with or without 24-h treatment of MG132 (10 μM). Inhibition of proteasomal activity by MG132 increased BK-β1 protein expression in diabetic vessels. *B*, robust BK channel openings by DHS-1 (0.1 μM) were observed in freshly isolated diabetic coronary SMCs after 12-h incubation with MG132. Group data with statistical analysis are shown in the *bar graphs*. *Dashed lines* represent the channel closed state (*c*). *W/O*, washout.

DISCUSSION

In this study, we made several novel findings. First, we found that MuRF1 was abundantly expressed in vascular SMCs and that the expression of MuRF1 was significantly up-regulated in diabetic vessels and under HG culture conditions as a result of increased NF-κB signaling. Second, MuRF1 interacted physically with BK-β1 and facilitated BK-β1 protein ubiquitination and degradation, leading to BK channelopathy and coronary vasculopathy in diabetes. Third, a co-IP assay demonstrated that the N terminus of BK-β1 and the coiled-coil region of MuRF1 were required for the formation of protein complexes. Fourth, overexpression of MuRF1 in the coronary arteries of non-diabetic mice mimicked the dysfunction of BK channels and coronary arteries of diabetic mice. Most importantly, knockdown of MuRF1 expression and pharmacological suppression of proteasome and NF-κB activities augmented BK-β1 expression and preserved vascular BK channel function in diabetes and hyperglycemia. Thus, we have provided compelling first evidence that impaired vascular BK channel function and coronary vasodilation in diabetes is associated with an increase of NF-κB/MuRF1-dependent BK-β1 degradation.

BK channel dysfunction promotes cardiovascular disorders, including hypertension, heart failure, myocardial infarction, stroke, retinopathy, and erectile dysfunction (45–48). Cardiovascular diseases are the leading cause of death in individuals with diabetes. The mechanisms that underlie diabetic vascular disorders are multifactorial. Besides endothelium dysfunction, abnormal smooth muscle function also critically contributes to vascular pathology in diabetes, especially under the long-term conditions of glucotoxicity and lipotoxicity (49). A major cause of diabetic BK channel abnormality is attributed to the down-regulation of BK-β1 expression in vascular SMCs (26, 27), resulting in impaired BK channel sensitivity to Ca^{2+} and voltage activation (26, 27). Many signaling pathways have been reported to be involved in the regulation of BK-β1 protein expression. For instance, it has been shown that the activation of calcineurin/nuclear factor of activated T-cells, cytoplasmic 3 (NFATC3) signaling suppressed vascular BK-β1 expression in angiotensin II-induced hypertensive mice (50). We have also reported previously that the down-regulation of BK-β1 expression in diabetes and under HG culture conditions is ubiquitin/proteasome-dependent (28). In our previous study, we have

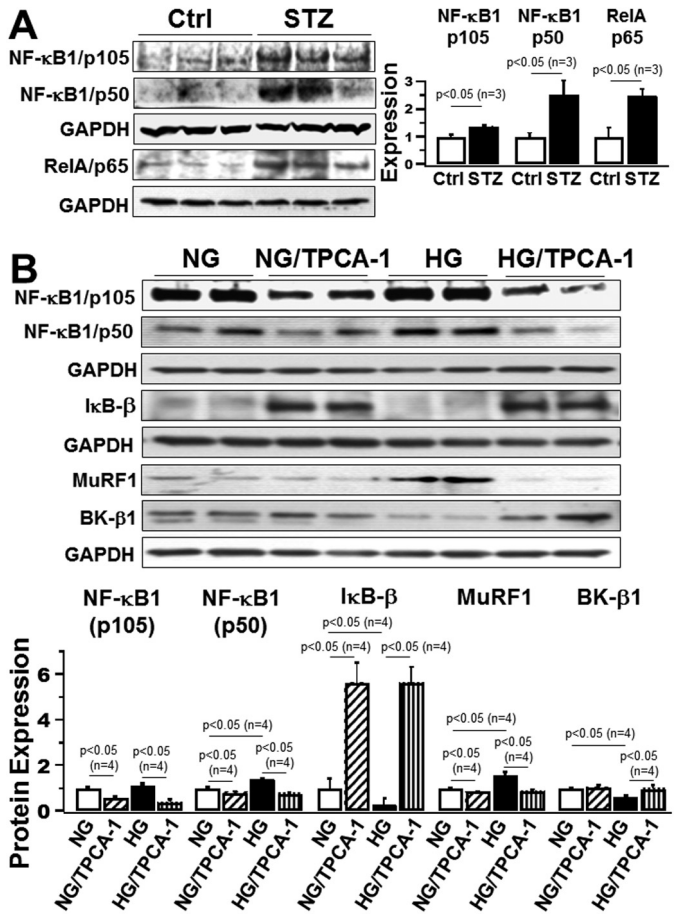

FIGURE 7. **Regulation of MuRF1 and BK-β1 expression by NF-κB.** *A*, protein expression of NF-κB1/p105, NF-κB1/p50, and RelA/p-65 in the aortas of control and STZ-induced diabetic mice. The levels of NF-κB/p105, NF-κB1/p50, and p-65 protein expression were significantly increased in diabetic mice compared with controls (*Ctrl*). *B*, 24-h incubation with 0.5 μM TPCA-1 suppressed the levels of NF-κB1/p105, NF-κB1/p50, and MuRF1 expression but markedly increased that of IκB-β in both NG- and HG-cultured human coronary SMCs. TPCA-1 treatment did not alter BK-β1 expression in NG-cultured cells but significantly enhanced that in HG-cultured cells. Group data and statistical analysis are shown in the *bar graphs*.

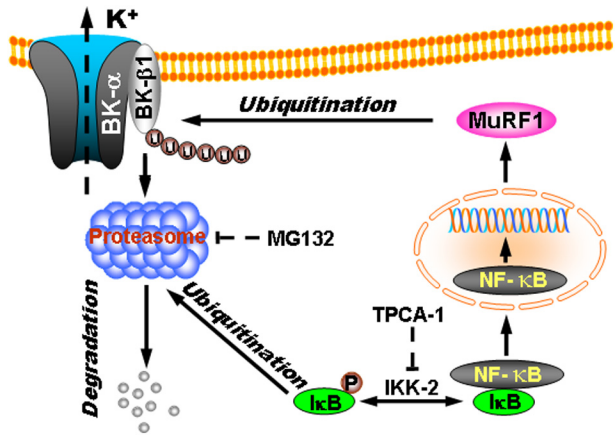

FIGURE 8. **A proposed model for NF-κB/MuRF1-dependent BK-β$_1$ protein degradation in diabetic vessels.** In diabetic vessels, increased NF-κB/p50 and p65 expression stimulates MuRF1 mRNA transcription and protein expression. The coiled-coil domain of MuRF1 interacts with the N terminus of BK-β1, which induces BK-β1 protein ubiquitination and degradation through the UPS and leads to diminished BK channel activation and coronary vasodilation. TPCA-1 inhibits IKK-2 activity, which decreases IκB phosphorylation and prevents its dissociation from NF-κB/p65, thereby down-regulating MuRF1 expression. MG132 inhibits proteasomal activity and reduces BK-β1 proteolysis.

found that atrogin-1, another E3, regulated BK-β1 expression through interaction with the PDZ-binding motif in BK-β1 that facilitated BK-β1 protein ubiquitination (28). Moreover, the expression of atrogin-1 in diabetic vessels was up-regulated by oxidative stress-mediated up-regulation of forkhead box O transcription factor-3a (Foxo3a)-dependent atrogin-1 mRNA transcription (31). Foxo3a activity is dependent on its subcellular localization. Inhibition of Akt signaling by oxidative stress leads to Foxo3a nuclear translocation and facilitates Foxo biological function (51, 52). In this study, we further demonstrated that MuRF1 expression was similarly increased in diabetic vessels and also contributed significantly to BK-β1 dysfunction. Interestingly, MuRF1 mRNA and protein are only expressed in vascular SMCs, whereas those of atrogin-1 can be detected in both vascular SMCs and the vascular endothelium (data not shown). The PDZ motif of BK-β1 is located at the extracellular loop, whereas the N terminus of BK-β1 is intracellular. Hence, interaction between atrogin-1 and BK-β1 must occur before BK-β1 transportation to the sarcolemmal membrane. It is worth emphasizing that UPS is presented in the centrosomes and cytoskeletal networks as well as the outer surface of the endoplasmic reticulum and that UPS-associated proteolysis can take place at different cell organelles, dependent on the location of E3 recognizing motifs of substrates (53, 54). An increase of both MuRF1 and atrogin-1 expression in diabetic vessels may synergistically accelerate BK-β1 protein degradation at different stages of protein metabolism and exacerbate BK channel-mediated vascular dysfunction in diabetes.

MuRF1 transcription is controlled by NF-κB (55). It is known that NF-κB activation is a key event for the initiation of cardiovascular pathogenesis in diabetes as a result of increased oxidative stress (56, 57). We found that the protein levels of the NF-κB1/p50 and p65 subunits were augmented in diabetic vessels and in HG-cultured human coronary SMCs. Pretreatment with the IKK-2 inhibitor TPCA-1 significantly increased IκB expression and reduced NF-κB/p50 expression in both NG- and HG-cultured human coronary SMCs, but the effects of TPCA-1 were more potent under HG culture conditions, which maintained BK-β1 expression in HG-cultured cells to the level of NG-cells. Hence, NF-κB/MuRF1/BK-β1 should be considered a potential therapeutic target for diabetic coronary dysfunction (Fig. 8).

The specificity of substrate degradation by the proteasome is dependent on the E3 ligase. It has been confirmed that the E3 ligase Nedd-4 interacts with the PY motifs in the C terminus of the cardiac voltage-gated Na^+ channel ($Na_v1.5$), the epithelial Na^+ channel, and the voltage gated K^+ channel and leads to channel ubiquitination and degradation (58–60). We found that Nedd-4 did not regulate BK-β1 expression even though there is a PY motif at the extracellular loop of BK-β (data not shown), suggesting that the three-dimensional protein folding is critical. Many regions of MuRF1 have been reported to be associated with substrate proteins. For instance, MuRF1 interacts with the hydrophobic amino acids of "Titin repeats" (61) and myosin heavy chain in skeletal muscles (62). The coiled-coil

region of MuRF1 is responsible for the binding of troponin I in cardiomyocytes (63). The MuRF family conserved region is required for the interaction with phospho-c-Jun in the heart (64). Using BK-β1 and MuRF1 truncation mutants and a co-IP assay, we have identified the functional domains for physical interaction between BK-β1 and MuRF1. The N terminus of BK-β1 is the only region that interacts with MuRF1. The counterparts in MuRF1 are more complicated. We believe that the coiled-coil region of MuRF1 is the structure required for recruiting BK-β1 to MuRF1 because BK-β1 can be detected in the pulldown of the MuRF1 coiled-coil region alone, but a direct protein binding experiment is required to further confirm our findings. Our results are similar to previous observations that the coiled-coil region is sufficient for MuRF1 binding to sarcomeric M-line titin and thick filament (63). Interestingly, partially deleting the RING finger domain or the family conserved region of MuRF1 interferes with the physical association with BK-β1. One explanation is that the RING finger domain and the MuRF1 family conserved region are also important for proper three-dimensional protein folding that allows the coiled-coil region to bind with the N terminus of BK-β1. How the RING finger domain and the family conserved region influence the interaction between MuRF1 and BK-β1 is currently unclear and needs further investigation using *in vitro* protein binding assays. Nevertheless, this is the first report that MuRF1 physically interacts with BK-β1, facilitates BK-β1 protein degradation, and impairs BK channel function in diabetic vessels. Inhibition of MuRF1 expression protects BK-β1 expression and vascular BK channel function and preserves coronary vasoreactivity in diabetes.

Acknowledgments—We thank Merck Research Laboratories (Merck & Co) for the gift of DHS-1.

REFERENCES

1. Fang, J., and Alderman, M. H. (2006) Impact of the increasing burden of diabetes on acute myocardial infarction in New York City. 1990–2000. *Diabetes* **55,** 768–773
2. Norhammar, A., Lindbäck, J., Rydén, L., Wallentin, L., Stenestrand, U., and Register of Information and Knowledge about Swedish Heart Intensive Care Admission (RIKS-HIA) (2007) Improved but still high short- and long-term mortality rates after myocardial infarction in patients with diabetes mellitus. A time-trend report from the Swedish Register of Information and Knowledge about Swedish Heart Intensive Care Admission. *Heart* **93,** 1577–1583
3. Bjarnegård, N., Arnqvist, H. J., Lindström, T., Jonasson, L., Jönsson, A., and Länne, T. (2009) Long-term hyperglycaemia impairs vascular smooth muscle cell function in women with type 1 diabetes mellitus. *Diab. Vasc. Dis. Res.* **6,** 25–31
4. Searls, Y. M., Loganathan, R., Smirnova, I. V., and Stehno-Bittel, L. (2010) Intracellular Ca^{2+} regulating proteins in vascular smooth muscle cells are altered with type 1 diabetes due to the direct effects of hyperglycemia. *Cardiovasc. Diabetol.* **9,** 8
5. Velmurugan, G. V., and White, C. (2012) Calcium homeostasis in vascular smooth muscle cells is altered in type 2 diabetes by Bcl-2 protein modulation of InsP3R calcium release channels. *Am. J. Physiol. Heart Circ. Physiol.* **302,** H124–134
6. Kawano, N., Emoto, M., Mori, K., Yamazaki, Y., Urata, H., Tsuchikura, S., Motoyama, K., Morioka, T., Fukumoto, S., Shoji, T., Koyama, H., Okuno, Y., Nishizawa, Y., and Inaba, M. (2012) Association of endothelial and vascular smooth muscle dysfunction with cardiovascular risk factors, vascular complications, and subclinical carotid atherosclerosis in type 2 diabetic patients. *J. Atheroscler. Thromb.* **19,** 276–284
7. Bruno, R. M., and Ghiadoni, L. (2013) Vascular smooth muscle function. Defining the diabetic vascular phenotype. *Diabetologia* **56,** 2107–2109
8. Rueda, A., Fernández-Velasco, M., Benitah, J. P., and Gómez, A. M. (2013) Abnormal Ca^{2+} spark/STOC coupling in cerebral artery smooth muscle cells of obese type 2 diabetic mice. *PloS ONE* **8,** e53321
9. Abello, N., Kerstjens, H. A., Postma, D. S., and Bischoff, R. (2009) Protein tyrosine nitration. Selectivity, physicochemical and biological consequences, denitration, and proteomics methods for the identification of tyrosine-nitrated proteins. *J. Proteome Res.* **8,** 3222–3238
10. Benham, C. D., and Bolton, T. B. (1986) Spontaneous transient outward currents in single visceral and vascular smooth muscle cells of the rabbit. *J. Physiol.* **381,** 385–406
11. Nelson, M. T., Cheng, H., Rubart, M., Santana, L. F., Bonev, A. D., Knot, H. J., and Lederer, W. J. (1995) Relaxation of arterial smooth muscle by calcium sparks. *Science* **270,** 633–637
12. Jaggar, J. H., Wellman, G. C., Heppner, T. J., Porter, V. A., Perez, G. J., Gollasch, M., Kleppisch, T., Rubart, M., Stevenson, A. S., Lederer, W. J., Knot, H. J., Bonev, A. D., and Nelson, M. T. (1998) Ca^{2+} channels, ryanodine receptors and Ca^{2+}-activated K^+ channels. A functional unit for regulating arterial tone. *Acta Physiol. Scand.* **164,** 577–587
13. Ledoux, J., Werner, M. E., Brayden, J. E., and Nelson, M. T. (2006) Calcium-activated potassium channels and the regulation of vascular tone. *Physiology* **21,** 69–78
14. Dunn, K. M., and Nelson, M. T. (2010) Calcium and diabetic vascular dysfunction. Focus on "Elevated Ca^{2+} asparklet activity during acute hyperglycemia and diabetes in cerebral arterial smooth muscle cells." *Am. J. Physiol. Cell Physiol.* **298,** C203–205
15. McManus, O. B., Helms, L. M., Pallanck, L., Ganetzky, B., Swanson, R., and Leonard, R. J. (1995) Functional role of the beta subunit of high conductance calcium-activated potassium channels. *Neuron* **14,** 645–650
16. Meera, P., Wallner, M., Jiang, Z., and Toro, L. (1996) A calcium switch for the functional coupling between α (hSlo) and β subunits (Kv,Ca β) of maxi K channels. *FEBS Lett.* **385,** 127–128
17. Xia, X. M., Ding, J. P., and Lingle, C. J. (1999) Molecular basis for the inactivation of Ca^{2+}- and voltage-dependent BK channels in adrenal chromaffin cells and rat insulinoma tumor cells. *J. Neurosci.* **19,** 5255–5264
18. Cox, D. H., and Aldrich, R. W. (2000) Role of the β1 subunit in large-conductance Ca^{2+}-activated K^+ channel gating energetics. Mechanisms of enhanced Ca^{2+} sensitivity. *J. Gen. Physiol.* **116,** 411–432
19. Hoshi, T., Tian, Y., Xu, R., Heinemann, S. H., and Hou, S. (2013) Mechanism of the modulation of BK potassium channel complexes with different auxiliary subunit compositions by the omega-3 fatty acid DHA. *Proc. Natl. Acad. Sci. U.S.A.* **110,** 4822–4827
20. Li, M., Zhang, Z., Koh, H., Lu, R., Jiang, Z., Alioua, A., Garcia-Valdes, J., Stefani, E., and Toro, L. (2013) The beta1-subunit of the MaxiK channel associates with the thromboxane A2 receptor and reduces thromboxane A2 functional effects. *J. Biol. Chem.* **288,** 3668–3677
21. Dick, G. M., and Sanders, K. M. (2001) (Xeno)estrogen sensitivity of smooth muscle BK channels conferred by the regulatory β1 subunit. A study of β1 knockout mice. *J. Biol. Chem.* **276,** 44835–44840
22. Nagar, D., Liu, X. T., and Rosenfeld, C. R. (2005) Estrogen regulates β 1-subunit expression in Ca^{2+}-activated K^+ channels in arteries from reproductive tissues. *Am. J. Physiol. Heart Circ. Physiol.* **289,** H1417–1427
23. Fernández-Fernández, J. M., Tomás, M., Vázquez, E., Orio, P., Latorre, R., Sentí, M., Marrugat, J., and Valverde, M. A. (2004) Gain-of-function mutation in the KCNMB1 potassium channel subunit is associated with low prevalence of diastolic hypertension. *J. Clin. Invest.* **113,** 1032–1039
24. Chen, Y., Salem, R. M., Rao, F., Fung, M. M., Bhatnagar, V., Pandey, B., Mahata, M., Waalen, J., Nievergelt, C. M., Lipkowitz, M. S., Hamilton, B. A., Mahata, S. K., and O'Connor, D. T. (2010) Common charge-shift mutation Glu65Lys in K^+ channel β 1-Subunit KCNMB1. Pleiotropic consequences for glomerular filtration rate and progressive renal disease. *Am. J. Nephrol.* **32,** 414–424
25. Yang, Y., Li, P. Y., Cheng, J., Mao, L., Wen, J., Tan, X. Q., Liu, Z. F., and Zeng, X. R. (2013) Function of BKCa channels is reduced in human vascular smooth muscle cells from Han Chinese patients with hypertension.

Hypertension **61,** 519–525
26. McGahon, M. K., Dash, D. P., Arora, A., Wall, N., Dawicki, J., Simpson, D. A., Scholfield, C. N., McGeown, J. G., and Curtis, T. M. (2007) Diabetes downregulates large-conductance Ca^{2+}-activated potassium β 1 channel subunit in retinal arteriolar smooth muscle. *Circ. Res.* **100,** 703–711
27. Lu, T., Ye, D., He, T., Wang, X. L., Wang, H. L., and Lee, H. C. (2008) Impaired Ca^{2+}-dependent activation of large-conductance Ca^{2+}-activated K^+ channels in the coronary artery smooth muscle cells of Zucker Diabetic Fatty rats. *Biophys. J.* **95,** 5165–5177
28. Zhang, D. M., He, T., Katusic, Z. S., Lee, H. C., and Lu, T. (2010) Muscle-specific F-box only proteins facilitate BK channel β 1 subunit downregulation in vascular smooth muscle cells of diabetes mellitus. *Circ. Res.* **107,** 1454–1459
29. Navedo, M. F., Takeda, Y., Nieves-Cintrón, M., Molkentin, J. D., and Santana, L. F. (2010) Elevated Ca^{2+} sparklet activity during acute hyperglycemia and diabetes in cerebral arterial smooth muscle cells. *Am. J. Physiol. Cell Physiol.* **298,** C211–220
30. Wang, R. X., Shi, H. F., Chai, Q., Wu, Y., Sun, W., Ji, Y., Yao, Y., Li, K. L., Zhang, C. Y., Zheng, J., Guo, S. X., Li, X. R., and Lu, T. (2012) Molecular mechanisms of diabetic coronary dysfunction due to large conductance Ca^{2+}-activated K^+ channel impairment. *Chin. Med. J.* **125,** 2548–2555
31. Lu, T., Chai, Q., Yu, L., d'Uscio, L. V., Katusic, Z. S., He, T., and Lee, H. C. (2012) Reactive oxygen species signaling facilitates FOXO-3a/FBXO-dependent vascular BK channel β 1 subunit degradation in diabetic mice. *Diabetes* **61,** 1860–1868
32. Powell, S. R. (2006) The ubiquitin-proteasome system in cardiac physiology and pathology. *Am. J. Physiol. Heart Circ. Physiol.* **291,** H1-H19
33. Li, W., Bengtson, M. H., Ulbrich, A., Matsuda, A., Reddy, V. A., Orth, A., Chanda, S. K., Batalov, S., and Joazeiro, C. A. (2008) Genome-wide and functional annotation of human E3 ubiquitin ligases identifies MULAN, a mitochondrial E3 that regulates the organelle's dynamics and signaling. *PloS ONE* **3,** e1487
34. Mrosek, M., Meier, S., Ucurum-Fotiadis, Z., von Castelmur, E., Hedbom, E., Lustig, A., Grzesiek, S., Labeit, D., Labeit, S., and Mayans, O. (2008) Structural analysis of B-Box 2 from MuRF1. Identification of a novel self-association pattern in a RING-like fold. *Biochemistry* **47,** 10722–10730
35. Willis, M. S., Ike, C., Li, L., Wang, D. Z., Glass, D. J., and Patterson, C. (2007) Muscle ring finger 1, but not muscle ring finger 2, regulates cardiac hypertrophy *in vivo*. *Circ. Res.* **100,** 456–459
36. Willis, M. S., Schisler, J. C., Li, L., Rodríguez, J. E., Hilliard, E. G., Charles, P. C., and Patterson, C. (2009) Cardiac muscle ring finger-1 increases susceptibility to heart failure *in vivo*. *Circ. Res.* **105,** 80–88
37. Chen, S. N., Czernuszewicz, G., Tan, Y., Lombardi, R., Jin, J., Willerson, J. T., and Marian, A. J. (2012) Human molecular genetic and functional studies identify TRIM63, encoding Muscle RING Finger Protein 1, as a novel gene for human hypertrophic cardiomyopathy. *Circ. Res.* **111,** 907–919
38. Hayden, M. S., and Ghosh, S. (2004) Signaling to NF-κB. *Gene Dev.* **18,** 2195–2224
39. Lecker, S. H., Goldberg, A. L., and Mitch, W. E. (2006) Protein degradation by the ubiquitin-proteasome pathway in normal and disease states. *J. Am. Soc. Nephrol.* **17,** 1807–1819
40. Lu, T., Zhang, D. M., Wang, X. L., He, T., Wang, R. X., Chai, Q., Katusic, Z. S., and Lee, H. C. (2010) Regulation of coronary arterial BK channels by caveolae-mediated angiotensin II signaling in diabetes mellitus. *Circ. Res.* **106,** 1164–1173
41. Lu, T., Katakam, P. V., VanRollins, M., Weintraub, N. L., Spector, A. A., and Lee, H. C. (2001) Dihydroxyeicosatrienoic acids are potent activators of Ca^{2+}-activated K^+ channels in isolated rat coronary arterial myocytes. *J. Physiol.* **534,** 651–667
42. Althaus, M., Bogdan, R., Clauss, W. G., and Fronius, M. (2007) Mechanosensitivity of epithelial sodium channels (ENaCs). Laminar shear stress increases ion channel open probability. *FASEB J.* **21,** 2389–2399
43. Lu, T., Hong, M. P., and Lee, H. C. (2005) Molecular determinants of cardiac K(ATP) channel activation by epoxyeicosatrienoic acids. *J. Biol. Chem.* **280,** 19097–19104
44. Chai, Q., Wang, X. L., Zeldin, D. C., and Lee, H. C. (2013) Role of caveolae in shear stress-mediated endothelium-dependent dilation in coronary arteries. *Cardiovasc. Res.* **100,** 151–159
45. Amberg, G. C., and Santana, L. F. (2003) Downregulation of the BK channel β 1 subunit in genetic hypertension. *Circ. Res.* **93,** 965–971
46. Wan, E., Kushner, J. S., Zakharov, S., Nui, X. W., Chudasama, N., Kelly, C., Waase, M., Doshi, D., Liu, G., Iwata, S., Shiomi, T., Katchman, A., D'Armiento, J., Homma, S., and Marx, S. O. (2013) Reduced vascular smooth muscle BK channel current underlies heart failure-induced vasoconstriction in mice. *FASEB J.* **27,** 1859–1867
47. Mori, A., Suzuki, S., Sakamoto, K., Nakahara, T., and Ishii, K. (2011) BMS-191011, an opener of large-conductance Ca^{2+}-activated potassium channels, dilates rat retinal arterioles *in vivo*. *Biol. Pharm. Bull.* **34,** 150–152
48. Werner, M. E., Zvara, P., Meredith, A. L., Aldrich, R. W., and Nelson, M. T. (2005) Erectile dysfunction in mice lacking the large-conductance calcium-activated potassium (BK) channel. *J. Physiol.* **567,** 545–556
49. Popov, D., and Constantinescu, E. (2008) Arterial smooth muscle cells dysfunction in hyperglycaemia and hyperglycaemia associated with hyperlipidaemia. From causes to effects. *Arch. Physiol. Biochem.* **114,** 150–160
50. Nieves-Cintrón, M., Amberg, G. C., Nichols, C. B., Molkentin, J. D., and Santana, L. F. (2007) Activation of NFATc3 down-regulates the β 1 subunit of large conductance, calcium-activated K^+ channels in arterial smooth muscle and contributes to hypertension. *J. Biol. Chem.* **282,** 3231–3240
51. Brunet, A., Park, J., Tran, H., Hu, L. S., Hemmings, B. A., and Greenberg, M. E. (2001) Protein kinase SGK mediates survival signals by phosphorylating the forkhead transcription factor FKHRL1 (FOXO3a). *Mol. Cell. Biol.* **21,** 952–965
52. Sandri, M., Sandri, C., Gilbert, A., Skurk, C., Calabria, E., Picard, A., Walsh, K., Schiaffino, S., Lecker, S. H., and Goldberg, A. L. (2004) Foxo transcription factors induce the atrophy-related ubiquitin ligase atrogin-1 and cause skeletal muscle atrophy. *Cell* **117,** 399–412
53. Werner, E. D., Brodsky, J. L., and McCracken, A. A. (1996) Proteasome-dependent endoplasmic reticulum-associated protein degradation. An unconventional route to a familiar fate. *Proc. Natl. Acad. Sci. U.S.A.* **93,** 13797–13801
54. Wójcik, C., and DeMartino, G. N. (2003) Intracellular localization of proteasomes. *Int. J. Biochem. Cell Biol.* **35,** 579–589
55. Waddell, D. S., Baehr, L. M., van den Brandt, J., Johnsen, S. A., Reichardt, H. M., Furlow, J. D., and Bodine, S. C. (2008) The glucocorticoid receptor and FOXO1 synergistically activate the skeletal muscle atrophy-associated MuRF1 gene. *Am. J. Physiol. Endocrinol. Metab.* **295,** E785–797
56. Lorenzo, O., Picatoste, B., Ares-Carrasco, S., Ramírez, E., Egido, J., and Tuñón, J. (2011) Potential role of nuclear factor κB in diabetic cardiomyopathy. *Mediators Inflamm.* 2011:652097
57. Mariappan, N., Elks, C. M., Sriramula, S., Guggilam, A., Liu, Z., Borkhsenious, O., and Francis, J. (2010) NF-κB-induced oxidative stress contributes to mitochondrial and cardiac dysfunction in type II diabetes. *Cardiovasc. Res.* **85,** 473–483
58. Abriel, H., Kamynina, E., Horisberger, J. D., and Staub, O. (2000) Regulation of the cardiac voltage-gated Na^+ channel (H1) by the ubiquitin-protein ligase Nedd4. *FEBS Lett.* **466,** 377–380
59. Staub, O., Gautschi, I., Ishikawa, T., Breitschopf, K., Ciechanover, A., Schild, L., and Rotin, D. (1997) Regulation of stability and function of the epithelial Na^+ channel (ENaC) by ubiquitination. *EMBO J.* **16,** 6325–6336
60. Ekberg, J., Schuetz, F., Boase, N. A., Conroy, S. J., Manning, J., Kumar, S., Poronnik, P., and Adams, D. J. (2007) Regulation of the voltage-gated K^+ channels KCNQ2/3 and KCNQ3/5 by ubiquitination. Novel role for Nedd4–2. *J. Biol. Chem.* **282,** 12135–12142
61. McElhinny, A. S., Kakinuma, K., Sorimachi, H., Labeit, S., and Gregorio, C. C. (2002) Muscle-specific RING finger-1 interacts with titin to regulate sarcomeric M-line and thick filament structure and may have nuclear functions via its interaction with glucocorticoid modulatory element

binding protein-1. *J. Cell. Biol.* **157,** 125–136
62. Fielitz, J., Kim, M. S., Shelton, J. M., Latif, S., Spencer, J. A., Glass, D. J., Richardson, J. A., Bassel-Duby, R., and Olson, E. N. (2007) Myosin accumulation and striated muscle myopathy result from the loss of muscle RING finger 1 and 3. *J. Clin. Invest.* **117,** 2486–2495
63. Kedar, V., McDonough, H., Arya, R., Li, H. H., Rockman, H. A., and Patterson, C. (2004) Muscle-specific RING finger 1 is a *bona fide* ubiquitin ligase that degrades cardiac troponin I. *Proc. Natl. Acad. Sci. U.S.A.* **101,** 18135–18140
64. Li, H. H., Du, J., Fan, Y. N., Zhang, M. L., Liu, D. P., Li, L., Lockyer, P., Kang, E. Y., Patterson, C., and Willis, M. S. (2011) The ubiquitin ligase MuRF1 protects against cardiac ischemia/reperfusion injury by its proteasome-dependent degradation of phospho-c-Jun. *Am. J. Pathol.* **178,** 1043–1058